IRAQI JOURNAL OF APPLIED PHYSICS
Vol. 22, No. 1, January-March 2026, pp. 12-18

Green Synthesis and Characterization of Bismuth Oxide Nanoparticles for Optoelectronic Applications

Edrees E. Khadeer [1]
Muhammad H. Shareef [1]
Mohanad H. Mohammed [2]

[1] Department of Physics, College of Science, University of Mosul, Mosul, 41200, IRAQ
[2] Nineveh Education Directorate, Ministry of Education, Mosul, 41200, IRAQ
* Corresponding author: mohannad.hazim1983@gmail.com

The green approach of synthesizing bismuth oxide nanoparticles using peppermint extract is an effective method of producing bismuth oxide nanoparticles at a very low cost and thus increasing its production. Thus, this method is very effective and promising and gives better results without damaging anyone and is thus very useful and beneficial. This method of green synthesis of bismuth oxide is quite effective and also gives better results. The optical studies showed high transparency in visible light and strong ultra-violet rays. The refractive index was seen to decrease rapidly and then become stable. Thus, this method is very promising and useful. The synthesized bismuth oxide nanoparticles also showed high stability. This method can be very effective and thus is beneficial and useful. The titration curves showed a peak at around 1500 a.u. Thus, this method is very effective and gives better results and is thus beneficial and useful. This approach is effective and gives better results and is thus beneficial and useful. The XRD studies showed indications of a tetragonally symmetrical crystal system with a crystallite size of about 58.06 nm. Thus, this method is beneficial and useful as it gives better results. The synthesized bismuth oxide nanoparticles showed stability

Keywords: Green synthesis; Bi_2O_3 nanoparticles; Peppermint extract; Optical properties
Received: 7 May 2025; Revised: 30 June 2025; Accepted: 7 July 2025; Published: 1 January 2026

1. Introduction

The biosynthesis of nanoparticles using plant extracts has revolutionized the synthesis of metal and metal oxide nanoparticles and offered an innovative solution to overcome the issues associated with conventional methods, as conventional methods have been challenging in terms of environmental hazards and high-energy consumption [1]. Biological fluids such as plants, bacteria, fungi, and yeasts, etc., have been used as natural reducing agents to synthesize metal and metal oxide nanoparticles, making biosynthesis an eco-friendly and cheaper option while fulfilling the criteria for sustainable development to reduce hazardous wastes and prevent climatic changes [2,3]. Various plant extracts of plant materials such as plant leaves, flowers, fruits, seeds, bark, and roots, among others, are composed of various constituents known collectively as phytoconstituents, which exhibit various medicinal aspects. These plant components exhibit a range of constituents, from flavonoids and phenolic derivatives, through alkaloids, terpenoids, to those containing protein [1,4,5]. The plant constituents, therefore, provide a further value-added role in addition to that of nanoparticle synthesis, as this component exhibits capping agent properties that regulate shape and diameter, through a reduction reaction to metal in various combinatorial roles [3]. The various nanoparticle types, such as metal oxide, have earned a unique place in choosing this component in nanoparticle synthesis due to its unique properties that qualify this component in various functions involving catalytic reaction, energy through renewable sources, and environment cleaning processes, notably through emission processes [6]. The bismuth oxide nanoparticle, i.e., Bi_2O_3, therefore, has earned a unique place due to its various properties, as discussed below [7-18]. These features make them highly desirable for advanced technological and environmental applications, including [19-31]:

1. In solid-oxide fuel cells (SOFCs), serving as efficient electrolytes for energy conversion.
2. In drug delivery systems, exploiting their visible-light photocatalytic activity for targeted therapy.
3. In antibacterial applications, effectively inhibiting pathogens like *E. coli* through photocatalytic mechanisms.
4. In water purification, removing toxic heavy metals such as chromium VI via adsorption and degradation.

The recent developments have also shown that the nanoparticles of Bi_2O_3 exhibit good absorption of UV light, with the performance of the nanoparticles being better compared to bulk materials due to their large surface area to volume ratio. Although conventional methods, including sol-gel [24], hydrothermal [21], laser ablation [22], and CVD [29], involve the use of hazardous chemicals that require large amounts of energy, the green synthesis method provides an alternative that is not only safe but also eco-friendly. The use of plant extracts replaces the use of hazardous chemicals [30-32].

In this paper, an efficient approach for the green synthesis of Bi_2O_3 nanoparticles using *Mentha pulegium*, which is also known as pennyroyal, has been proposed based on its high content of active compounds that can induce efficient reduction and stabilization of the synthesized nanoparticles. The potentiality of the synthesized nanoparticles has been assessed based on the comprehensive analysis of their structural and optical properties. This paper is considered a significant improvement in the green synthesis of nanoparticles and their potential applications in different areas of the environment.

2. Experimental Methods

Fresh leaves of *Mentha pulegium* (peppermint) were cleaned properly using double distilled water for the removal of impurities. Then the leaves were dried under the shade to avoid the photochemical degradation of the bioactive compounds. Then the leaves were powdered using an electric grinder. For the preparation of the extract, 10 g of the powdered leaves was refluxed using 100 mL of double distilled water at 90°C for 2 hours using a magnetic stirrer. Then the liquid extract was cooled at room temperature and filtered using Whatman No.1 filter paper. Then the liquid extract was centrifuged at 4000 rpm for 30 minutes. For the synthesis of nanoparticles, 2 g of pure bismuth nitrate pentahydrate crystal, which is denoted by $Bi(NO_3)_3{\cdot}5H_2O$ and has 99.98% purity, was dissolved in 10 ml of deionized water at 90°C. Then, the solution was mixed with 20 ml of peppermint extract using magnetic stirring at 500 rpm at 90°C for 18 hours. The volume of the solution was kept constant during the heating process. Finally, the nanoparticles, as shown in Fig. (1), confirm the synthesis of bismuth oxide nanoparticles using the eco-friendly approach.

Fig. (1) The solution of Bi_2O_3 nanoparticles

Bismuth oxide (Bi_2O_3) thin films were deposited on preheated glass substrates at 300°C by using the spray pyrolysis method in an ambient atmosphere. The precursor solution was atomized and evenly sprayed on the substrate by using the spray pyrolysis method with precise control over the flow rate. A heat-resistant collector was placed at the bottom of the spray nozzle to prevent the accumulation of the solution and hence any defects in the thin films. After the deposition, the substrate was cooled for 30 minutes. This helped in the complete oxidation and crystallization of the thin films without any cracking. In this manner, high-quality Bi_2O_3 thin films were obtained with maximum integrity. The structural properties of the synthesized Bi_2O_3 nanoparticles were analyzed by using a SHIMADZU XRD-6000 diffractometer, which was employed by using CuKα radiation with a wavelength of 1.54060 Å at 40 kV and 30 mA to analyze the phase and crystallography properties. The morphological properties of the synthesized nanoparticles were analyzed by using a Nova NanoSEM 450 field-emission scanning electron microscope (FE-SEM).

The optical properties of the Bi_2O_3 thin films were characterized using a Caihong 721-1000 single-beam UV-Visible spectrophotometer. The baseline correction was done by measuring the blank substrate before measuring the samples. The absorption spectrum obtained from the measurement can be used to determine the band gap energy and analyze the light interaction properties of the material.

3. Results and Discussion

The crystal structure of the bismuth oxide thin film was investigated using the XRD technique. The XRD pattern was obtained between 5° and 85°, which corresponds to the 2θ values. The XRD pattern, as shown in Fig. (2), indicated that the diffraction pattern of the bismuth oxide thin film was characterized by distinct peaks corresponding to the (220), (240), (402), (006), and other planes. The highest peak was observed at 2θ= 23.44° corresponding to the (220) plane. The well-separated peaks indicated that the bismuth oxide thin film was in the polycrystalline state. The bismuth oxide thin film was found to be tetragonal, β-Bi_2O_3, using the Mach3 software by comparing the diffraction pattern with the standard JCPDS card (96-900-7724), which indicated good agreement.

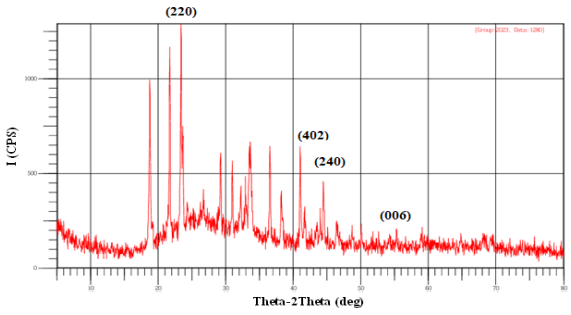

Fig. (2) XRD pattern of Bi_2O_3 nanoparticles

The average crystallite size of the bismuth oxide nanoparticles was found to be 58.06 nm using the Debye-Scherrer formula: $D=K\lambda/\beta cos\theta$ [37]. In the

calculation, the shape factor (K) of 0.91, Cu-Kα radiation (λ=1.54060Å), and the full-width at half maximum (β) of the (220) diffraction peak in radians were used. The XRD analysis clearly indicates the successful preparation of nanomaterials, and the average crystallite size indicates the formation of highly ordered nanocrystals.

From the morphological studies carried out on the substrate using scanning electron microscopy at 5 kx and 10 kx magnification, it is observed that the substrate surface is homogeneous and consists of uniformly dispersed nanograins, as seen in Fig. (3). The granular nanostructure is highly correlated to the tetragonal polycrystalline phase, and thus conclusive evidence is obtained regarding the formation of β-Bi_2O_3 nanoparticles. The experimental results obtained in the present work are highly correlated to the experimental results reported in the literature by Motakef-Kazemi and Yaqoubi [2], validating the reliability of the fabrication process.

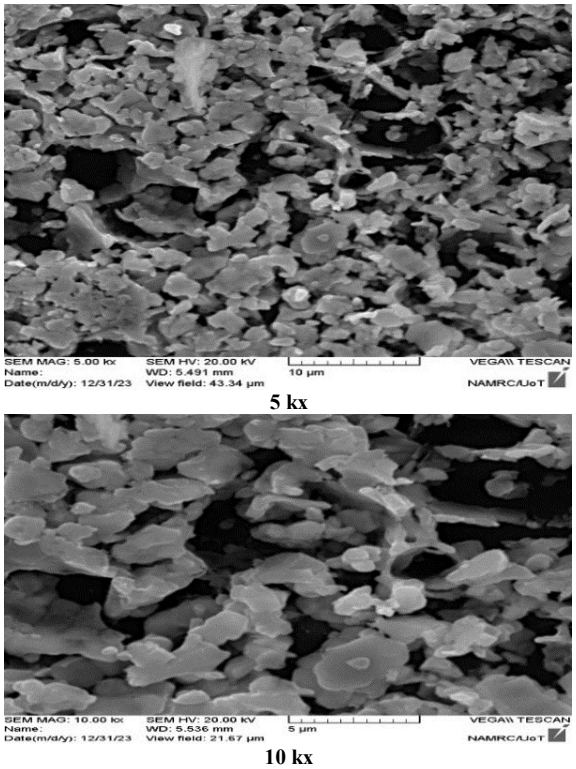

Fig. (3) Scanning electron microscope (SEM) images of Bi_2O_3 nanoparticles at two different magnifications

The UV-Visible spectroscopic analysis of the synthesized bismuth oxide thin film, as depicted in Fig. (4a), showed that there was the presence of distinct absorption peaks in the range from 320 to 1000 nm. The absorption spectrum of the synthesized bismuth oxide thin film showed that there was a distinct absorption peak in the UV region between 320 and 400 nm, close to the fundamental absorption peak. The absorption spectrum was also present up to 550 nm in the visible region. The reduction in the absorption intensity with the increase in the wavelength can be attributed to the limitations set by the band gap, where the energy of the incident photons was not sufficient to allow the transition of the electrons. The absorption spectrum reached a plateau at a wavelength much longer than 770 nm, indicating that the near-infrared region was reached. The above findings showed that the properties of the synthesized thin film were that of a wide band gap semiconductor material, which can be used in the development of photovoltaic cells, especially in the range of [38]:

1. High absorption of UV-Visible radiation in the range from 320 to 550 nm,
2. Infrared transparency,
3. The performance of the material will depend on its implementation. The implementation can be in the form of transparent conducting oxides in front electrodes or active absorber layers in hetero junctions.

The material has the potential to be used in the next generation of solar cells, which will be able to absorb the visible region of the solar spectrum and be transparent in the infrared region.

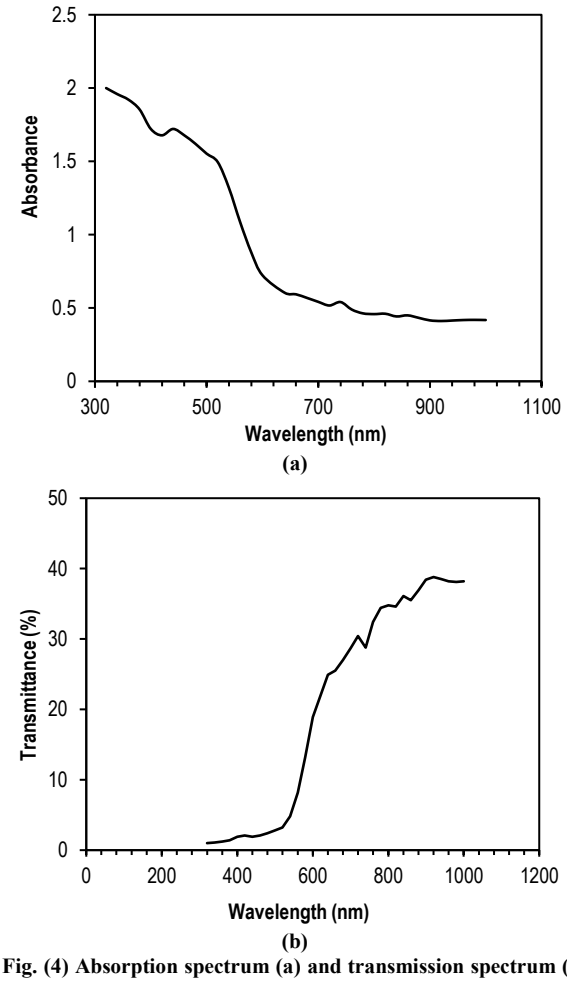

Fig. (4) Absorption spectrum (a) and transmission spectrum (b) of Bi_2O_3 thin film as a function of wavelength

The transmission spectrum of the bismuth oxide thin film has an inverse relation to its absorption spectrum. The transmittance of the bismuth oxide thin film is very low at its fundamental absorption edge in the range of the shorter wavelengths. The transmittance of the bismuth oxide thin film increases sharply with the increase in wavelength until it reaches a plateau in the near infrared region for wavelengths above 900 nm.

This large difference in the behavior of the material, i.e., efficient absorption of visible light and high transmittance in the infrared region, again emphasizes the good potential of the material for solar cell applications. Such behavior in the material is highly desirable for solar cell applications because the efficient absorption of visible light and the low loss of energy in the form of non-absorbable infrared radiation are of primary importance. The results obtained in this work are in good agreement with the nature of the wide bandgap semiconductor material.

The reflectance (R) of the bismuth oxide thin film, which is the fraction of the energy of incident radiation that reflects off the thin film, was determined using the principle of energy conservation, where R = 1–A–T, and A and T are the absorbance and transmittance, respectively [39]. As shown in Fig. (5), the reflectance spectrum gradually decreased within the range of 320-1000 nm, which indicates that the reflectance is inversely proportional to the absorption and transmission. For example, at low wavelengths, the absorption was predominant, and the reflectance was high due to the interaction of the incident photons with matter. At longer wavelengths, the transmission was predominant, and the reflectance was low. This change in reflectance also shows that the material has a wavelength dependency in its optical properties and that it is a promising material for the development of photonic devices using the reflection of light.

The optical band gap value of the prepared thin film of bismuth oxide was determined using the Tauc method from the Davis-Mott equation for direct transitions, which is expressed by the following equation: $(\alpha h\nu)^2 = B[h\nu - E_g]$ [40], where the absorption coefficient is expressed by the following equation: $\alpha = 2.303A/t$ (where t is the film thickness = 4.815×10^{-5} m), B is a constant, and E_g, which is the band gap.

As shown in Fig. (6), the band gap is found by extrapolating the straight part of the curve to the point where it intersects the x-axis, or where $(\alpha h\nu)^2 = 0$. The analysis was done to find the direct allowed transitions, where n = 2. As shown in the figure, it is an accurate method for the determination of the optoelectronic properties of the semiconductor, thus proving the suitability of the thin film for use in photonic devices. The linear region of the Tauc plot also proves the quality and integrity of the thin film.

The optical bandgap energy of the bismuth oxide nanoparticles was determined to be 2.4 eV, which makes it a semiconductor. The optical bandgap energy is an indication that the material has promising optoelectronic properties. The material has an intermediate optical bandgap energy, meaning that it is neither an insulator nor a semiconductor. This was indicated by the Tauc plot analysis. The 2.4 eV optical bandgap energy indicates that the material can absorb blue-green light, which has a wavelength of 515 nm. This material can be used for various applications in the visible region. This has been supported by various recent studies on the properties of Bi_2O_3 nanoparticles that have been synthesized using green synthesis methods, as reported in the study by Motakef-Kazemi and Yaqoubi [2]. The study reported that the direct bandgap energy of Bi_2O_3 nanoparticles was determined to be 2.4 eV. This study was consistent with our findings regarding the UV-Visible absorption properties, where the material was found to be transparent in the infrared region and to absorb visible light in the range of 320-520 nm.

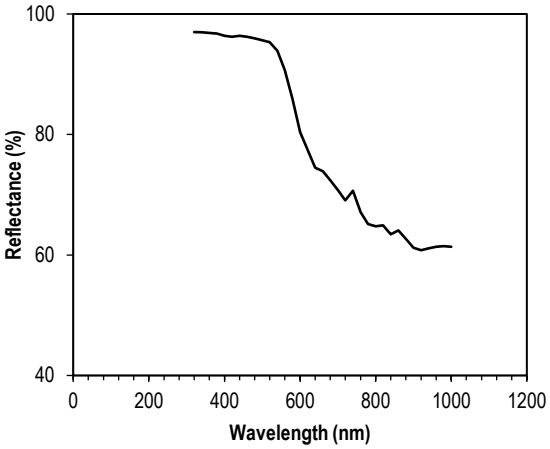

Fig. (5) Variation of reflectance of Bi_2O_3 thin film as a function of wavelength

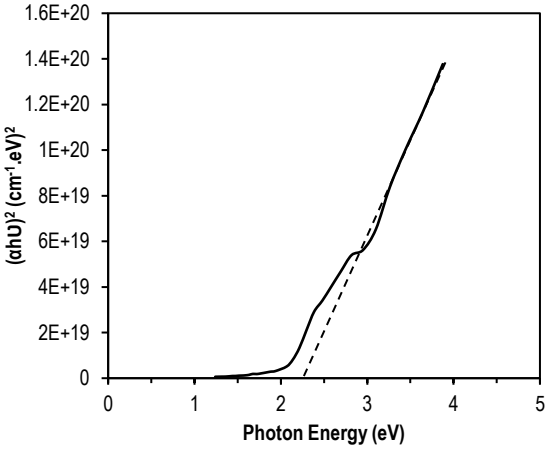

Fig. (6) Variation of $(\alpha h\nu)^2$ of Bi_2O_3 thin film as a function of photon energy ($h\nu$)

Though the former has been the subject matter of the research works presented in the past, the similarity

in the optical and structural properties of the materials synthesized by various authors ensures the reproducibility of the plant-mediated synthesis of Bi_2O_3. The optical properties of the Bi_2O_3 film have provided valuable information regarding the interaction of matter with light. Figure (7a) represents the plot that shows the extinction coefficient of the Bi_2O_3 film. The equation representing the extinction coefficient is given by the equation $k=\alpha\lambda/4\pi$, where α represents the absorption coefficient and λ represents the wavelength of the incident radiation [41]. The extinction coefficient of the Bi_2O_3 film has been found to show a sharp peak at 1500 a.u. in the range of the wavelength between 400 and 450 nm. The extinction coefficient represents the absorption of the incident radiation by the material due to band-to-band transitions at the absorption edge. The extinction coefficient decreases gradually with an increase in the wavelength between 520 and 1000 nm.

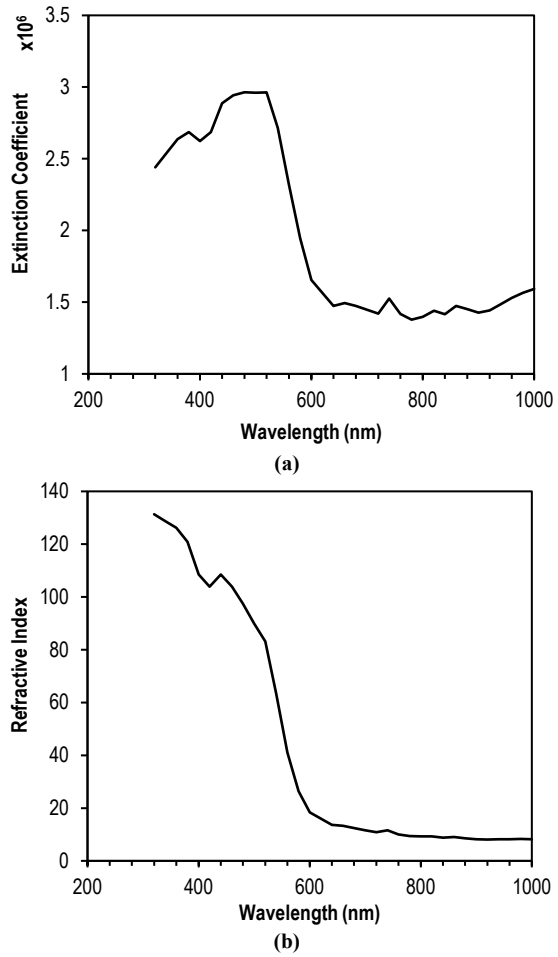

Fig. (7) Variation of extinction coefficient (k) and refractive index (n) of Bi_2O_3 thin film as functions of wavelength

Another way to analyze the refractive index, using the equation $n=(1+k)/(1-k)$, also indicates normal characteristics of dispersion. It is observed that, as shown in Fig. (7b), there is a significant decrease in the refractive index in the visible region, followed by stability in the near-infrared (NIR) region. This is the normal behavior of wide band gap semiconductors. Again, the strong correlation observed between the variations of k and n with wavelength indicates the band gap energy of the film to be 2.4 eV, along with the high absorption efficiency of the film in the visible region (400-600 nm), which is transparent to near-infrared (NIR) light. Again, the reproducibility of the values of the refractive index of the film indicates the high quality of the nanostructured Bi_2O_3 film, which is useful for optoelectronics in the visible region.

4. Conclusion

The green-synthesized bismuth oxide (Bi_2O_3) nanoparticles were found to have a polycrystalline tetragonal phase with an average crystallite size of 58.06 nm. These nanoparticles have dense nano-granular form with uniform distribution on the substrate. The nanoparticles showed excellent absorption for ultraviolet light, and the maximum absorbance was in the range of 320-400 nm. The nanoparticles also showed high reflectance, around 70%, between 320 and 500 nm. The green-synthesized Bi_2O_3 nanoparticles were found to have direct bandgap of 2.4 eV, high absorbance in the visible region and high transmittance in the infrared region.

Acknowledgment

The authors sincerely thank the University of Mosul, College of Science, for their financial support and access to essential research facilities, which were instrumental in achieving the objectives of this study.

References

[1] H.H. Azeez, H.H. Hasan and H.H. Karim, "Green Synthesis ZnO NPs and Their Effects on Plant Growing", *Coll. Basic Edu. Res. J.*, 20(2.1) (2024) 103.

[2] N. Motakef-Kazemi and M. Yaqoubi, "Green synthesis and characterization of bismuth oxide nanoparticle using Mentha pulegium extract", *Iranian J. Pharmaceut. Res.,* 19 (2020) 70-79.

[3] U. Shanker, C.M. Hussain and M. Rani, **"Green nanomaterials for industrial applications"**, Elsevier (2022).

[4] S.A. Aromal and D. Philip, "Green synthesis of gold nanoparticles using Trigonella foenum-graecum and its size-dependent catalytic activity", *Spectrochim. Acta A*, 97 (2012) 1–5.

[5] F. Tavakoli, M. Salavati-Niasari and F. Mohandes, "Green synthesis and characterization of graphene nanosheets", *Mater. Res. Bull.*, 63 (2015) 51-57.

[6] P. Falcaro et al., "Application of metal and metal oxide nanoparticles@MOFs", *Coord. Chem. Rev.*, 307 (2016) 237–254.

[7] V. Mane et al., "A review on Bi_2O_3 nanomaterial for photocatalytic and antibacterial applications", *Chem. Phys. Impact*, 8 (2024) 100517.
[8] H.T. Fan et al., "δ-Bi_2O_3 thin films prepared by reactive sputtering: Fabrication and characterization", *Thin Solid Films*, 513 (20066) 142–147.
[9] W. Raza et al., "Synthesis, characterization and photocatalytic performance of visible light-induced bismuth oxide nanoparticle", *J. Alloys Compd.*, 648 (2015) 641–650.
[10] Y. Gong et al., "Performance of (La,Sr)MnO_3 cathode-based solid oxide fuel cells: Effect of bismuth oxide sintering aid in silver paste cathode current collector", *J. Power Sources*, 196 (2011) 928–934.
[11] X. Gou et al., "Room-temperature solution synthesis of Bi_2O_3 nanowires for gas sensing application", *Nanotech.,* 20 (2009) 495–501.
[12] P. Malik and D. Chakraborty, "Bi_2O_3-catalyzed oxidation of aldehydes with t-BuOOH", *Tetrahedron Lett.*, 51 (2010) 3521–3523.
[13] F. Xia et al., "Preparation of bismuth nanoparticles in aqueous solution and catalytic performance for the reduction of 4-nitrophenol", *Ind. Eng. Chem. Res.*, 53 (2014) 10576–10582.
[14] M. Schlesinger et al., "Metastable β-Bi_2O_3 nanoparticles with potential for photocatalytic water purification using visible light irradiation", *Chemistry*, 2 (2013) 146–155.
[15] W.E. Mahmoud and A.A. Al-Ghamdi, "Synthesis and properties of bismuth oxide nanoshell-coated polyaniline nanoparticles for promising photovoltaic properties", *Polym. Adv. Technol.*, 22 (2011) 877–881.
[16] M.J. Oviedo et al., "New bismuth germanate oxide nanoparticle material for biolabel applications in medicine", *J. Nanomater.*, 2016 (2016) https://doi.org/10.1155/2016/9782625.
[17] A.M.N. Jassim et al., "Study the antibacterial effect of bismuth oxide and tellurium nanoparticles", *Int. J. Chem. Biol. Sci.*, 1 (2015) 81–84.
[18] N. Nurmalasari, Y. Yulizar and D.O.B. Apriandanu, "Bi_2O_3 nanoparticles: Synthesis, characterizations, and photocatalytic activity", Department of Chemistry, Faculty of Mathematics and Natural Sciences (FMIPA), Universitas Indonesia, Depok 16424, Indonesia. doi: 10.1088/1757-899X/763/1/012036.
[19] J. La et al., "Synthesis of bismuth oxide nanoparticles by solution combustion method", *Particul. Sci. Technol.*, 31 (2012) 287–290.
[20] J. Wu et al., "Solvothermal synthesis of uniform bismuth nanospheres using poly(N-vinyl-2-pyrrolidone) as a reducing agent", *Nanoscale Res. Lett.*, 6 (2011) 66–74.
[21] Z.A. Zulkifli et al., "Synthesis and characterisation of bismuth oxide nanoparticles using hydrothermal method: The effect of reactant concentrations and application in radiotherapy", *J. Phys. Conf. Ser.*, (2018) doi: 10.1088/1742-6596/1082/1/012103.
[22] M.H. Mohammed, M.N. Hussein and A.K.A. Suleiman, "Effect of Deposition Method on Optical and Structural Properties of Bismuth Oxide Thin Films", *Iraqi J. Appl. Phys.*, 21(1) (2025) 71-74.
[23] S. Anandan and J.J. Wu, "Microwave-assisted rapid synthesis of Bi_2O_3 short nanorods", *Mater. Lett.*, 63 (2009) 2387–2389.
[24] M. Mallahi et al., "Synthesis and characterization of bismuth oxide nanoparticles via sol-gel method", *Adv. J. Eng. Res.*, 3 (2014) 162–165.
[25] L. Mädler and S.E. Pratsinis, "Bismuth oxide nanoparticles by flame spray pyrolysis", *J. Am. Ceram. Soc.*, 85 (2004) 1713–1718.
[26] G. Carotenuto et al., "Synthesis and thermoelectric characterisation of bismuth nanoparticles", *J. Nanopart. Res.*, 11 (2009) 1729–1738.
[27] T.P. Gujar et al., "Formation of highly textured (111) Bi_2O_3 films by anodization of electrodeposited bismuth films", *Appl. Surf. Sci.*, 252 (2006) 2747–2751.
[28] T.P. Gujar, V.R. Shinde and C.D. Lokhande, "The influence of oxidation temperature on structural, optical and electrical properties of thermally oxidized bismuth oxide films", *Appl. Surf. Sci.*, 254 (2008) 4186–4190.
[29] R.Z.A. Al-Fulayih et al., "Preparation of CdTe thin films using seed method", *Func. Mater.*, 31(3) (2024) 377-380.
[30] P. Nazari et al., "Biosynthesis of bismuth nanoparticles using *Serratia marcescens* isolated from the Caspian Sea and their characterization", *IET Nanobiotechnol.*, 6 (2012) 58–62.
[31] S. Mondal et al., "Biogenic synthesis of Ag, Au and bimetallic Au/Ag alloy nanoparticles using aqueous extract of mahogany (Swietenia mahogani JACQ.) leaves", *Colloid Surf. B*, 82 (2011) 497–504.
[32] R. Dobrucka, "Synthesis of titanium dioxide nanoparticles using *Echinacea purpurea Herba*", *Iran. J. Pharma. Res.*, 16 (2017) 753–759.
[33] R. Senthamilselvi and R. Velavan, "Microstructure and photocatalytic properties of bismuth oxide (Bi_2O_3) nanocrystallites", *Malaya J. Matematik*, 2 (2020) 4870–4874.
[34] N. Motakef-Kazemi and M. Yaqoubi, "Green synthesis and characterization of bismuth oxide nanoparticle using *Mentha pulegium* extract", *Iranian J. Pharma. Res.,* 19 (2020) 70-79.
[35] A. Becheri et al., "Synthesis and characterization of zinc oxide nanoparticles: Application to

textiles as UV-absorbers", *J. Nanoparticle Res.*, 10 (2008) 679–689.
[36] Y.M. Im et al., "Effect of ZnO nanoparticles morphology on UV blocking of poly(vinyl alcohol)/ZnO composite nanofibers", *Mater. Lett.*, 147 (2015) 20–24.
[37] A.A. Sulaiman, "Effect of γ-Irradiation on the n-Porous Silicon Structures Prepared by Electrochemical Etching", *Rafidain J. Sci.*, 27(3) (2018) 173-180.
[38] K. Yoshikawa et al., "Silicon heterojunction solar cell with interdigitated back contacts for a photoconversion efficiency over 26%", *Nat. Energy*, 2 (2017) 17032.
[39] M. Al-Azow et al., "Preparation of Silver Nanoparticles By Nd:YAG Pulsed Laser and Study Their Optical and Structural Properties", *J. Edu. Sci.*, 34(2) (2025) 13-23.
[40] E.E. Ghadeer, R.Z.A. Al-Fulayih and Z.B. Ibraheem, "Study of the effect of adding glass and carbon powders on optical behavior of unsaturated polyester resin", *AIP Conf. Proc.*, 2394 (2022) 090023.
[41] E.E. Khadeer, M.A. Abed and M.A. Hmood, "The Optical Properties of Unsaturated Polyester Reinforcement by Glass Fibers", *Jordan J. Phys.*, 17(2) (2024) 155-163.

